Article

# ScN@C: Encapsulated Cluster Regiocontrol of Adduct Docking on an Ellipsoidal Metallofullerene Sphere

Ting Cai, Liaosa Xu, Harry W. Gibson, Harry C. Dorn, Christopher J. Chancellor, Marilyn M. Olmstead, and Alan L. Balch

*J. Am. Chem. Soc.*, **2007**, 129 (35), 10795-10800• DOI: 10.1021/ja072345o • Publication Date (Web): 10 August 2007



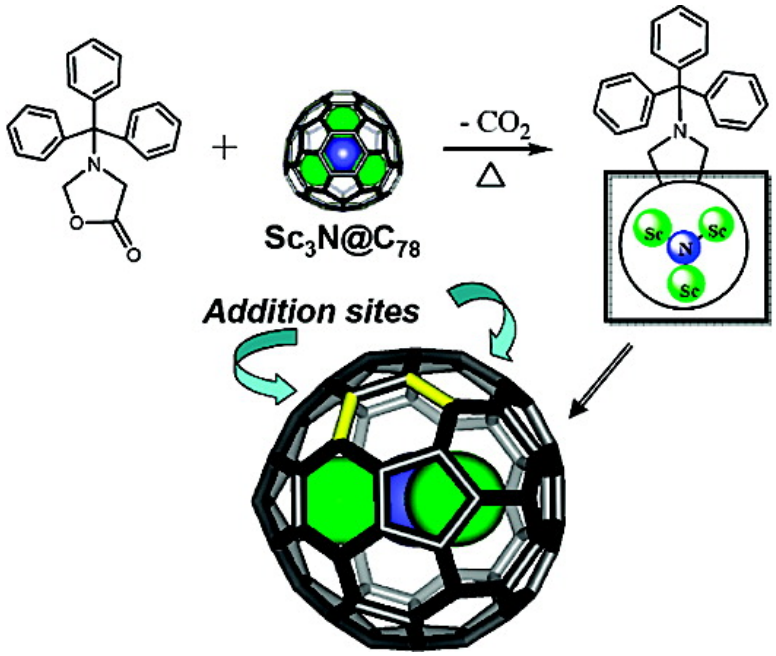


## More About This Article

Additional resources and features associated with this article are available within the HTML version:

- Supporting Information
- Links to the 8 articles that cite this article, as of the time of this article download
- Access to high resolution figures
- Links to articles and content related to this article
- Copyright permission to reproduce figures and/or text from this article

View the Full Text HTML

J|A|C|S
ARTICLES
Published on Web 08/10/2007

# $Sc_3N@C_{78}$: Encapsulated Cluster Regiocontrol of Adduct Docking on an Ellipsoidal Metallofullerene Sphere

Ting Cai,[†] Liaosa Xu,[†] Harry W. Gibson,*[,†] Harry C. Dorn,*[,†]
Christopher J. Chancellor,[‡] Marilyn M. Olmstead,[‡] and Alan L. Balch*[,‡]

*Contribution from the Departments of Chemistry, Virginia Polytechnic Institute and State University, Blacksburg, Virginia 24060-0212, and University of California, Davis, California 95616*

Received April 3, 2007; E-mail: hdorn@vt.edu; hwgibson@vt.edu; albalch@ucdavis.edu

***Abstract:*** The first *N*-tritylpyrrolidino derivatives of $D_{3h}$ (78:5) $Sc_3N@C_{78}$ were successfully synthesized and isolated. The addition sites for the two nearly equivalent kinetic monoadducts **1a** and **1b** are across two different 6,6 junction sites on the $Sc_3N@C_{78}$ cage that are offset from the horizontal plane defined by the $Sc_3N$ cluster. The adducts were characterized by NMR experiments, DFT calculations and X-ray crystallographic analysis of $Sc_3N@C_{78}$ derivative **1a**. A unique finding of this study is the regiocontrol of adduct docking by the internal $Sc_3N$ cluster.

## Introduction

The chemistry of endohedral metallofullerenes has developed rapidly during the past decade, driven by the remarkable chemical and physical features that could provide many important applications in nanomaterials and biomedical science.[1−6] Since their discovery in 1999,[7] a large variety of trimetallic nitride templated endohedral metallofullerenes (TNT EMFs) with different encapsulated metals, cage sizes, and symmetries have been synthesized and isolated.[7−16] After the initial discovery of the TNT EMF class represented by the prototypical $Sc_3N@C_{80}$ ($I_h$ cage),[7] $Sc_3N@C_{78}$ was also discovered and X-ray crystallographic analysis revealed that it possesses $D_{3h}$ (78:5) symmetry (Figure 1).[9] Both crystallography and DFT calculations of $Sc_3N@C_{78}$ show that the scandium atoms are localized over the three pyracylene patches.[9,17] Studies on the electronic and vibrational structures of $Sc_3N@C_{78}$ suggest that there are strong interactions between the $Sc_3N$ cluster and the fullerene cage carbon atoms.[18,19] Specifically, the $Sc_3N$ unit is constrained to the horizontal plane of the $D_{3h}$ (78:5) cage because of the more ellipsoidal character of this cage. Two other $C_{78}$ endohedral metallofullerenes, $La_2@C_{78}$[20] and $Ti_2C_2@C_{78}$,[21,22] were reported

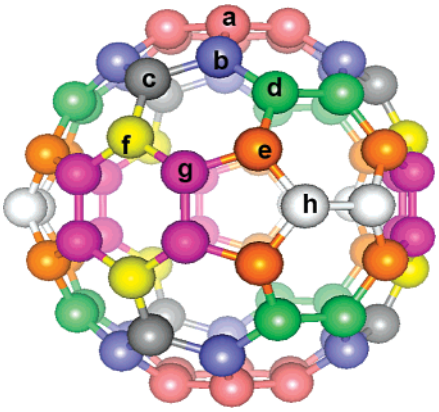


***Figure 1.*** Schematic diagram of the carbon cage of the $D_{3h}$ (78:5) $C_{78}$ isomer showing the eight bands of different types of carbon atoms. The three-fold axis is aligned vertically, and the horizontal mirror plane passes through the h-type carbon atoms. There are two $D_{3h}$ isomers of $C_{78}$ that obey the isolated pentagon rule. Throughout this article we are concerned only with the specific isomer (78:5) shown here.[9]

[†] Virginia Polytechnic Institute and State University.
[‡] University of California, Davis.

(1) Thilgen, C.; Diederich, F. *Chem. Rev.* **2006**, *106*, 5049−5135.
(2) Martin, N. *Chem. Commun.* **2006**, 2093−2104.
(3) Shinohara, H. *Rep. Prog. Phys.* **2000**, *63*, 843−892.
(4) *Endofullerenes: A New Family of Carbon Clusters*; Akasaka, T., Nagase, S., Eds.; Kluwer: Dordrecht, The Netherlands, 2002.
(5) Cagle, D. W.; Kennel, S. J.; Mirzadeh, S.; Alford, J. M.; Wilson, L. J. *Proc. Natl. Acad. Sci. U.S.A.* **1999**, *96*, 5182−5187.
(6) Kato, H.; Kanazawa, Y.; Okumura, M.; Taninaka, A.; Yokawa, T.; Shinohara, H. *J. Am. Chem. Soc.* **2003**, *125*, 4391−4397.
(7) Stevenson, S.; Rice, G.; Glass, T.; Harich, K.; Cromer, F.; Jordan, M. R.; Craft, J.; Hadju, E.; Bible, R.; Olmstead, M. M.; Maitra, K.; Fisher, A. J.; Balch, A. L.; Dorn, H. C. *Nature* **1999**, *401*, 55−57.
(8) Stevenson, S.; Fowler, P. W.; Heine, T.; Duchamp, J. C.; Rice, G.; Glass, T.; Harich, K.; Hajdu, E.; Bible, R.; Dorn, H. C. *Nature* **2000**, *408*, 427−428.
(9) Olmstead, M. H.; de Bettencourt-Dias, A.; Duchamp, J. C.; Stevenson, S.; Marciu, D.; Dorn, H. C.; Balch, A. L. *Angew. Chem., Int. Ed.* **2001**, *40*, 1223−1225.
(10) Iezzi, E. B.; Duchamp, J. C.; Fletcher, K. R.; Glass, T. E.; Dorn, H. C. *Nano Lett.* **2002**, *2*, 1187−1190.
(11) Stevenson, S.; Phillips, J. P.; Reid, J. E.; Olmstead, M. M.; Rath, S. P.; Balch, A. L. *Chem. Commun.* **2004**, 2814−2815.
(12) Krause, M.; Wong, J.; Dunsch, L. *Chem. Eur. J.* **2005**, *11*, 706−711.
(13) Yang, S. F.; Dunsch, L. *J. Phys. Chem. B* **2005**, *109*, 12320−12328.
(14) Cai, T.; Xu, L.; Anderson, M. R.; Ge, Z.; Zuo, T.; Wang, X.; Olmstead, M. M.; Balch, A. L.; Gibson, H. W.; Dorn, H. C. *J. Am. Chem. Soc.* **2006**, *128*, 8581−8589.
(15) Wang, X.; Zuo, T.; Olmstead, M. M.; Duchamp, J. C.; Glass, T. E.; Cromer, F.; Balch, A. L.; Dorn, H. C. *J. Am. Chem. Soc.* **2006**, *128*, 8884−8889.
(16) Beavers, C. M.; Zuo, T.; Duchamp, J. C.; Harich, K.; Dorn, H. C.; Olmstead, M. M.; Balch, A. L. *J. Am. Chem. Soc.* **2006**, *128*, 11352−11353.
(17) Campanera, J. M.; Bo, C.; Olmstead, M. M.; Balch, A. L.; Poblet, J. M. *J. Phys. Chem. A* **2002**, *106*, 12356−12364.
(18) Krause, M.; Popov, A.; Dunsch, L. *ChemPhysChem* **2006**, *7*, 1734−1740.
(19) Park, S. S.; Liu, D.; Hagelberg, F. *J. Phys. Chem. A* **2005**, *109*, 8865−8873.
(20) Cao, B. P.; Wakahara, T.; Tsuchiya, T.; Kondo, M.; Maeda, Y.; Rahman, G. M. A.; Akasaka, T.; Kobayashi, K.; Nagase, S.; Yamamoto, K. *J. Am. Chem. Soc.* **2004**, *126*, 9164−9165.

to have the same $D_{3h}$ (78:5) symmetry. $Tm_3N@C_{78}$, $Dy_3N@C_{78}$ (I), and $Dy_3N@C_{78}$ (II) were also isolated and characterized.[12,13] Compared with $D_{3h}$ (78:5) $Sc_3N@C_{78}$, $Tm_3N@C_{78}$, $Dy_3N@C_{78}$ (I), and $Dy_3N@C_{78}$ (II) have significantly longer chromatographic retention times and distinct absorption spectra that suggest different cage structures for these cases.[12,13]

Functionalization of the TNT EMFs is necessary to provide unique nanomaterials useful for various future applications, for example, MRI contrast agents.[23] However, organic functionalization chemistry of $Sc_3N@C_{78}$ has not been extensively explored because only small amounts of the material were previously available. Recently, by taking advantage of the high kinetic stability of TNT EMFs, it has been found that high purity TNT EMFs can be obtained directly from soot or its extract by selectively trapping empty cage fullerenes and classic EMFs on a functionalized support, yielding only the more stable TNT EMFs $Sc_3N@C_{68}$, $Sc_3N@C_{78}$, and $Sc_3N@C_{80}$.[24,25] This breakthrough makes it possible to isolate significant quantities of $Sc_3N@C_{78}$ utilizing a single chromatographic step in a relatviely short period of time.

In this paper, we report the synthesis and characterization of the first *N*-tritylpyrrolidino derivatives of $D_{3h}$ (78:5) $Sc_3N@C_{78}$ utilizing the Prato reaction.[26,27] These results are compared with previous studies of the homologous $Sc_3N@C_{80}$, both in terms of chemical reactivity and regioselectivity, as well as crystallographic studies. Ellipsoidal $Sc_3N@C_{78}$ $D_{3h}$ (78:5) represents a case where the internal trimetallic cluster ($Sc_3N$) is restricted to a horizontal plane allowing exploration of the regiocontrol of exohedral adduct docking on a metallofullerene sphere.

## Results and Discussion

Recently, pyrrolidino derivatives of icosahedrally symmetric ($I_h$) $Sc_3N@C_{80}$ were synthesized via 1,3-dipolar cycloaddition of azomethine ylides to the fullerene cage and characterized.[28−30] A kinetic study showed that the 6,6-ring junction adduct is the kinetically controlled product; it is converted to the thermodynamic product, the 5,6-ring junction adduct, upon thermal equilibration.[30−32] On the other hand, the minor $Sc_3N@C_{80}$ isomer, with $D_{5h}$ symmetry, exhibits higher reactivity in the Prato reaction with the tritylazomethine ylide in comparison with the $I_h$ analogue and yields the thermodynamically stable monoadduct by addition across the 6,6-ring junction of a pyracylene unit.[14]


(21) Yumura, T.; Sato, Y.; Suenaga, K.; Iijima, S. *J. Phys. Chem. B* **2005**, *109*, 20251−20255.
(22) Tan, K.; Lu, X. *Chem. Commun.* **2005**, 4444−4446.
(23) Fatouros, P. P.; Corwin, F. D.; Chen, Z. J.; Broaddus, W. C.; Tatum, J. L.; Kettenmann, B.; Ge, Z.; Gibson, H. W.; Russ, J. L.; Leonard, A. P.; Duchamp, J. C.; Dorn, H. C. *Radiology* **2006**, *240*, 756−764.
(24) Ge, Z.; Duchamp, J. C.; Cai, T.; Gibson, H. W.; Dorn, H. C. *J. Am. Chem. Soc.* **2005**, *127*, 16292−16298.
(25) Stevenson, S.; Harich, K.; Yu, H.; Stephen, R. R.; Heaps, D.; Coumbe, C.; Phillips, J. P. *J. Am. Chem. Soc.* **2006**, *128*, 8829−8835.
(26) Maggini, M.; Scorrano, G.; Prato, M. *J. Am. Chem. Soc.* **1993**, *115*, 9798−9799.
(27) Prato, M.; Maggini, M. *Acc. Chem. Res.* **1998**, *31*, 519−526.
(28) Cardona, C. M.; Kitaygorodskiy, A.; Ortiz, A.; Herranz, M. A.; Echegoyen, L. *J. Org. Chem.* **2005**, *70*, 5092−5097.
(29) Cai, T.; Ge, Z.; Iezzi, E. B.; Glass, T. E.; Harich, K.; Gibson, H. W.; Dorn, H. C. *Chem. Commun.* **2005**, 3594−3596.
(30) Cai, T.; Slebodnick, C.; Xu, L.; Harich, K.; Glass, T. E.; Chancellor, C.; Fettinger, J. C.; Olmstead, M. M.; Balch, A. L.; Gibson, H. W.; Dorn, H. C. *J. Am. Chem. Soc.* **2006**, *128*, 6486−6492.
(31) Cardona, C. M.; Elliott, B.; Echegoyen, L. *J. Am. Chem. Soc.* **2006**, *128*, 6480−6485.
(32) Rodriguez-Fortea, A.; Campanera, J. M.; Cardona, C. M.; Echegoyen, L.; Poblet, J. M. *Angew. Chem., Int. Ed.* **2006**, *45*, 8176−8180.


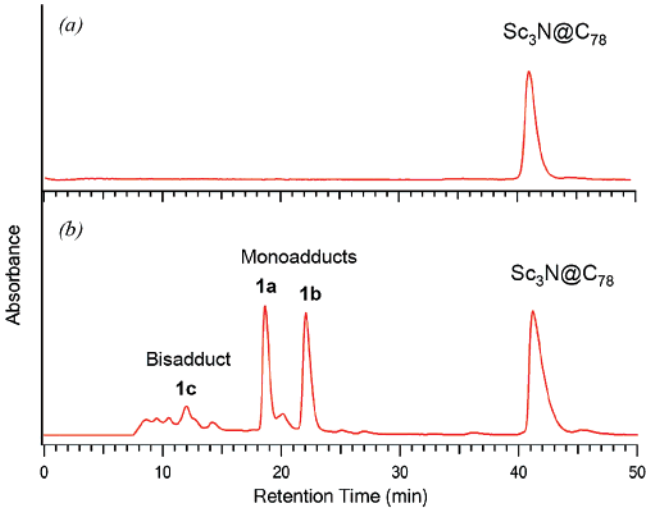


***Figure 2.*** HPLC chromatograms of (a) the initial $Sc_3N@C_{78}$, and (b) the product mixture from the Prato reaction. HPLC conditions: 10 × 250 mm PYE [2-(1′-pyrenyl)ethyl silica] column at 2.0 mL $min^{-1}$ flow rate with toluene, 390 nm detection.

***Scheme 1.*** The Prato Reaction of $Sc_3N@C_{78}$ with *N*-Triphenylmethyl-5-oxazolidinone

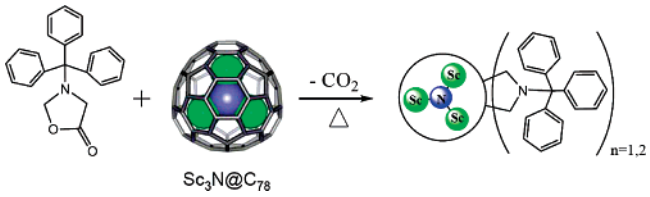


In the present work, two mono- and one di-*N*-tritylpyrrolidino $Sc_3N@C_{78}$ derivatives were obtained after a 3 h reflux with *N*-trityloxazolideneone in chlorobenzene (Scheme 1 and Figure 2). From high performance liquid chromatography (HPLC) of the reaction mixture (Figure 2), product **1a** (18.6 min) and **1b** (22.0 min) were identified as the monoadducts by MALDI-TOF MS (Figure 3a,b). A small quantity of bisadduct **1c** was also isolated and characterized by MALDI-TOF MS (Figure 3c). The molecular ion peak of bisadduct **1c** was observed at *m*/*z* 1656. The fragment peak at *m*/*z* 1373 was due to loss of one of the tritylpyrrolidino groups. The fragment peaks at *m*/*z* 1413 and *m*/*z* 1128 resulted from the loss of the trityl groups from tritylpyrrolidino groups of **1c**, as expected on the basis of the high stability of the trityl cation. Complete loss of both tritylpyrrolidino groups gave the $Sc_3N@C_{78}$ ion fragment peak at *m*/*z* 1085. The shorter retention time of the bisadduct **1c** (12.0 min) is analogous to bisadducts of the $I_h$ and $D_{5h}$ isomers of $Sc_3N@C_{80}$.[14,30] However, the reactivity of $Sc_3N@C_{78}$ is significantly higher than $Sc_3N@C_{80}$ $I_h$ based on the reaction rate for the monoadducts and higher yields of bisadducts in a shorter time period.[30]

The $^{13}C$ NMR spectrum of **1a** (with $^{13}C$-enriched methylene carbon atoms in the pyrrolidine ring by use of $^{13}C$ labeled starting material) exhibits peaks at 59.3 and 67.3 ppm, indicating that methylene carbon atoms $C_a$ and $C_b$ are nonequivalent (Figure 4a). The $^1H$ NMR spectrum of **1a** contains two triplets (at 3.79 and 3.31 ppm) for the methylene hydrogens $H_a$ and $H_b$ (triplets due to coupling with adjacent $^{13}C$ labeled methylene carbon, $^1J_{C-H} = 141$ Hz). The heteronuclear multiple quantum coherence (HMQC) spectrum confirms the assignment; the

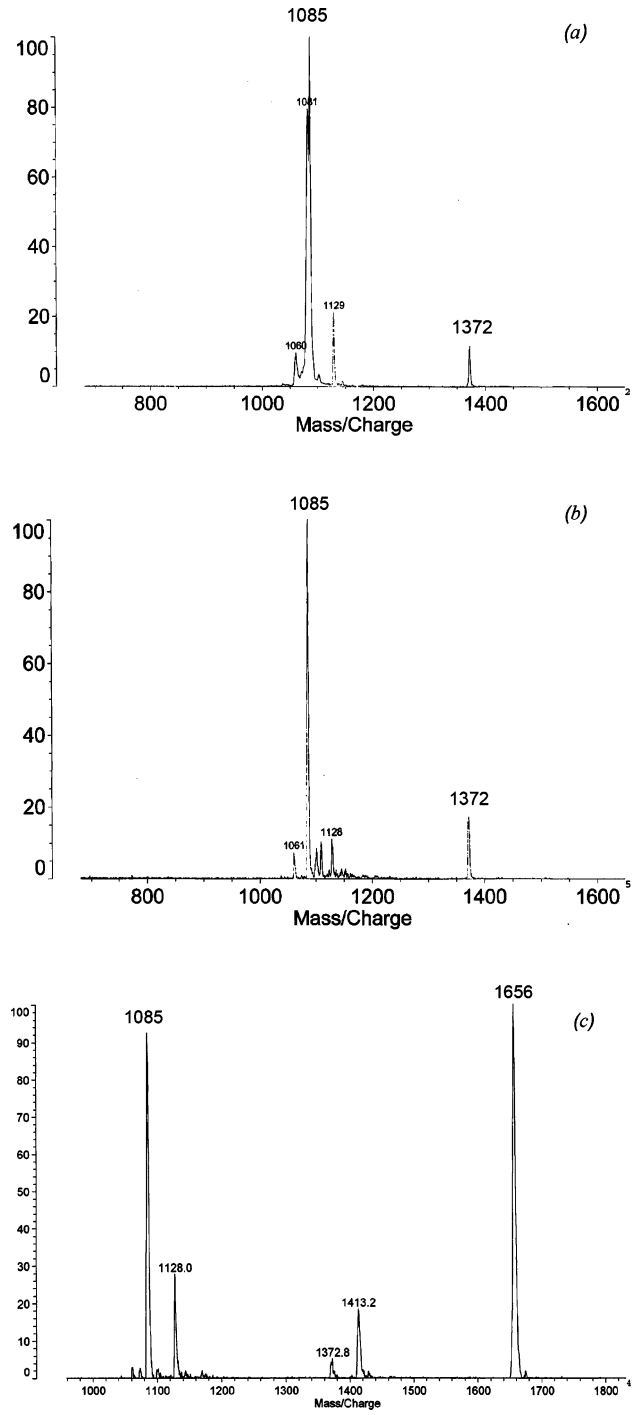


***Figure 3.*** Matrix-assisted laser desorption ionization time-of-flight (MALDI-TOF) mass spectra using a 9-nitroanthracene matrix and negative ionization: (a) monoadduct **1a**, (b) monoadduct **1b**, (c) bisadduct **1c**. Calculated for monoadducts, *m*/*z* 1372; calculated for bisadducts, *m*/*z* 1655.

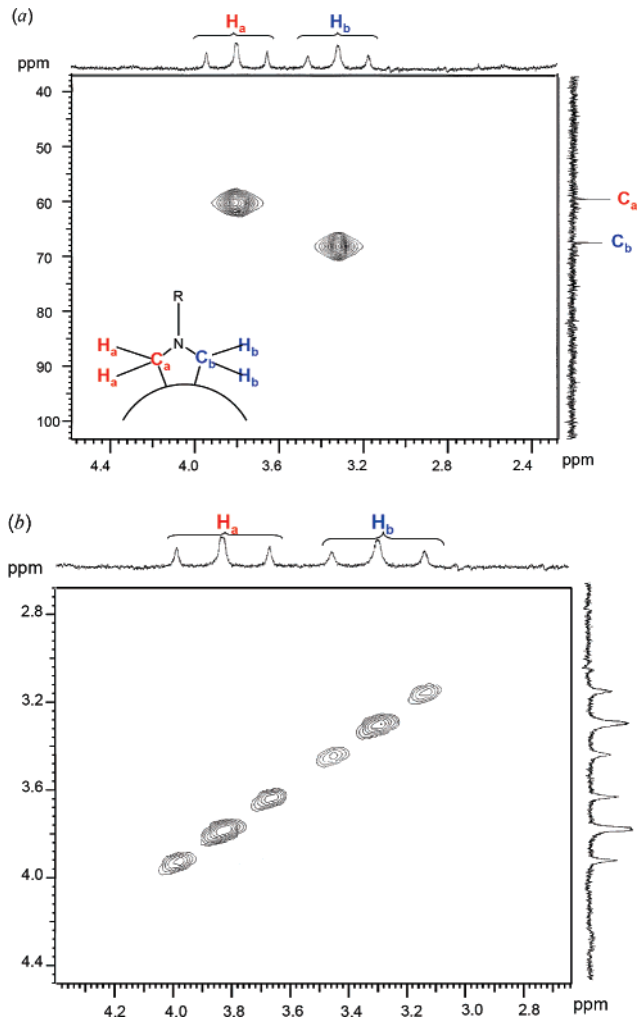


***Figure 4.*** 500 MHz (a) HMQC and (b) COSY spectra of the $Sc_3N@C_{78}$ *N*-tritylpyrrolidino monoadducts **1a** [solvent: 1,2-dichlorobenzene-$d_4$].

methylene carbon atoms $C_a$ and $C_b$ are coupled to the adjacent methylene hydrogen atoms $H_a$ and $H_b$, respectively (Figure 4a). The correlation spectroscopy (COSY) spectrum (Figure 4b) confirms that these methylene protons are not coupled. In addition, based on previous studies with the pyrrolidino metallofullerene derivatives, differential shielding effects from pentagon−hexagon ring currents on the surface cage and the nitrogen atom of the pyrrolidine ring, the 5,6-ring junction adduct always exhibits large chemical shift differences (1.2−1.4 ppm) for the diastereotopic methylene protons of the pyrrolidine ring.[28−30,33] In contrast, the 6,6-junction adducts have either no or much smaller shift differences (~0.2 ppm).[14,30,33,34] Therefore, we conclude that **1a** is a 6,6-ring junction adduct with equivalent methylene protons (assuming rapid inversion of the pyrrolidine ring) but nonequivalent methylene carbons.

The $^{13}C$ NMR spectrum of **1b** (with $^{13}C$-enriched methylene carbons in the pyrrolidine ring by use of $^{13}C$ labeled starting material) exhibits peaks at 56.2 and 66.8, indicating nonequivalent methylene carbon atoms $C_a$ and $C_b$. In the $^1H$ NMR spectrum of **1b** (Figure 5a), the geminal methylene hydrogen atoms on each carbon are also nonequivalent in contrast to **1a** in which the geminal methylene hydrogens on each carbon are equivalent. The HMQC spectrum of **1b** shows that $H_a$ (3.24 ppm) and $H_{a'}$ (3.07 ppm) are coupled with $C_a$, and $H_b$ (3.16 ppm) and $H_{b'}$ (3.05 ppm) couple with $C_b$. The $H_a-H_{a'}$ and $H_b-H_{b'}$ couplings are confirmed by the COSY spectrum (Figure 5b). Therefore, we conclude that **1b** is also a 6,6-ring junction adduct, but with both nonequivalent methylene carbons and hydrogens.

(33) Yamada, M.; Wakahara, T.; Nakahodo, T.; Tsuchiya, T.; Maeda, Y.; Akasaka, T.; Yoza, K.; Horn, E.; Mizorogi, N.; Nagase, S. *J. Am. Chem. Soc.* **2006**, *128*, 1402−1403.
(34) Cardona, C. M.; Kitaygorodskiy, A.; Echegoyen, L. *J. Am. Chem. Soc.* **2005**, *127*, 10448−10453.

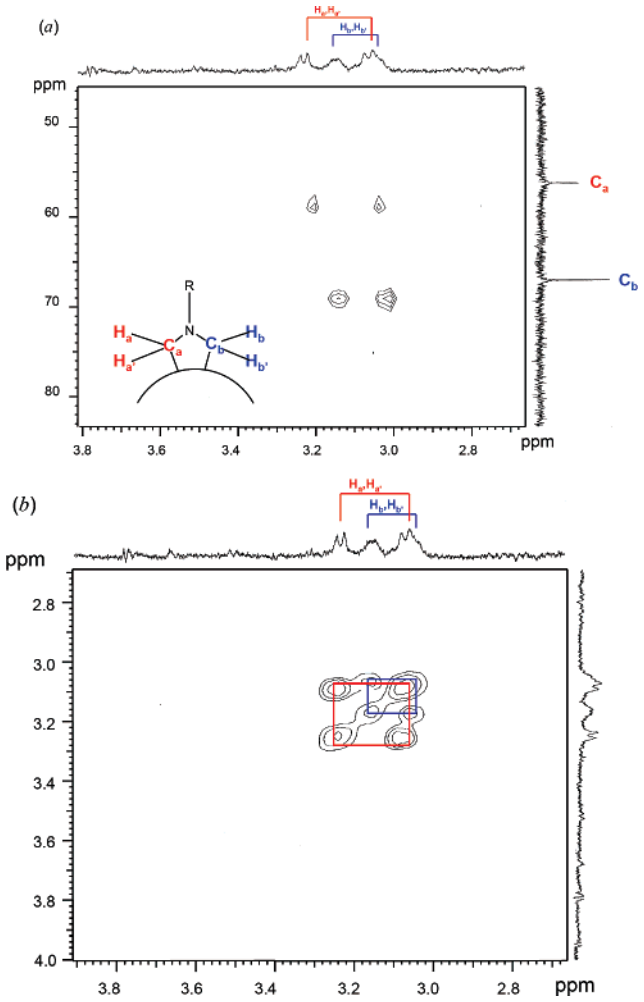


***Figure 5.*** 500 MHz (a) HMQC and (b) COSY spectra of the $Sc_3N@C_{78}$ *N*-tritylpyrrolidino monoadducts **1b**. For good resolution, methylene carbons are not $^{13}C$-enriched in the 1D proton spectrum of **1b** [solvent: 1,2-dichlorobenzene-$d_4$].

***Table 1.*** Comparison of Symmetries for $D_{3h}$ (78:5) $Sc_3N@C_{78}$ *N*-Tritylpyrrolidino Monoadducts at Different Addition Sites

| site of addition | ring junction type | number of equivalent bonds | symmetry of the methylene carbon atoms | symmetry of the methylene hydrogen atoms |
|---|---|---|---|---|
| a-a | 6,6 | 6 | symmetric | symmetric |
| a-a | 6,5 | 6 | symmetric | symmetric |
| a-b | 6,5 | 12 | asymmetric | asymmetric |
| b-c | 6,5 | 12 | asymmetric | asymmetric |
| b-d | 6,6 | 12 | asymmetric | asymmetric |
| d-d | 6,6 | 6 | symmetric | asymmetric |
| d-e | 6,6 | 12 | asymmetric | asymmetric |
| g-e | 6,5 | 12 | asymmetric | asymmetric |
| c-f | 6,6 | 6 | asymmetric | symmetric |
| f-g | 6,6 | 12 | asymmetric | asymmetric |
| g-g | 6,5 | 6 | symmetric | asymmetric |
| h-h | 6,6 | 3 | symmetric | symmetric |

The $D_{3h}$ (78:5) ellipsoidal $Sc_3N@C_{78}$ carbon cage has 8 different types of carbon atoms and 13 sets of C−C bonds as shown in Figure 1. The statistical numbers of bonds of each type, the type of ring junction involved and the symmetry of the addition patterns are summarized in Table 1. As suggested by the NMR data for **1a**, the c-f bond is the only possible 6,6-ring junction reaction site that produces nonequivalent methylene carbon atoms but equivalent geminal methylene protons. The reaction site for **1b**, based in Table 1 and the NMR data, has three possibilities: the b-d, d-e, and f-g bonds; these three sites yield 6,6-ring junction adducts with both nonequivalent methylene carbon atoms and hydrogen atoms. DFT calculations were performed for the three **1b** adducts as well as pristine $Sc_3N@C_{78}$ and $Sc_3N@C_{80}$. Consistent with the observed higher reactivity of $Sc_3N@C_{78}$ the HOMO−LUMO gap (2.24 eV) is significantly lower than for pristine $I_h$ $Sc_3N@C_{80}$ (2.56 eV). For the three **1b** adducts, the b-d bond adduct has a significantly lower relative thermodynamic energy (~20 kcal/mol) and larger HOMO−LUMO gap (0.4−0.6 eV) than those of the d-e and f-g bond adducts (Table 2). However, the differences in the relative thermodynamic energies and the HOMO−LUMO gaps for the b-d bond adduct and c-f adduct **1a** are quite small (2.1 kcal/mol and 0.04 eV), accounting for the experimental observed production of two kinetically favored monoadducts. Therefore, d-e and f-g bond sites can be ruled out, and we suggest that the b-d bond is the most likely addition site for the monoadduct **1b**. Consistent with our calculations and experimental result, Campanera et al. also suggested that the c-f and b-d bond are the two most reactive site in pristine $Sc_3N@C_{78}$ based on the higher Mayer Bond Order (MBO) values (Table 2) compared with other bond sites.[35]

Black crystals of **1a** suitable for single-crystal X-ray diffraction were obtained by evaporation of a benzene solution. Figure 6 shows two drawings of the adduct. The upper drawing shows a view in which the flat $Sc_3N$ unit lies in the horizontal plane. This view looks down what would have been the three-fold axis of the parent $Sc_3N@C_{78}$. The lower drawing shows a clearer view of the attachment of the addend to the cage. Addition has occurred at a c-f bond in the endohedral fullerene and this adduct addition site is above but equidistant from the Sc3 and Sc1 atoms that define the plane of the $Sc_3N$ unit. Thus, three pyracylene patches in the plane of the $Sc_3N$ unit and the h-type carbon atoms are not susceptible to external attack. Thus, the addend avoids any interaction with the $Sc_3N$ unit, which remains in the horizontal plane of the $C_{78}$ cage. The Sc−N distances are Sc1−N1 2.001(2), Sc2−N1 1.999(2), and Sc3−N1 2.001(2) Å. The Sc−N distances are similar to those in other endohedrals containing the planar $Sc_3N$ unit.[36]

The scandium ion resides at the center of a pyracylene patch in the middle of the $C_{78}$ cage. The shortest Sc−C distances are as follows: Sc1−C27, 2.213(3); Sc1−C28, 2.271(3); Sc2−C34, 2.238(3); Sc2−C35, 2.250(3); Sc3−C42, 2.210(3); Sc3−C41 2.269(3) Å. The positioning of the metal ions within the $C_{78}$ cage corresponds to that seen in the parent endohedral metallofullerene. However, in that structural study which involved the cocrystal, $Sc_3N@C_{78}\cdot Co^{II}(OEP)\cdot 1.5C_6H_6\cdot 0.3CHCl_3$, there were three different orientations of the cage and three orientation of the $Sc_3N$ unit to consider. The present structure does not display any disorder.

The variations seen in the C−C distances in the $C_{78}$ cage are larger than those seen in $Sc_3N@C_{80}$ where there are only two types of C−C bonds with corresponding distances of 1.437(15) Å at the 5:6 ring junctions and 1.421(18) Å at the 6,6 ring junctions.[36] In **1a** the average C−C distances for the shortest C−C bonds are 1.394 Å for the a-a bonds at 6,6 ring junctions

(35) Campanera, J. M.; Bo, C.; Poblet, J. M. *J. Org. Chem.* **2006**, *71*, 46−54.
(36) Lee, H. M.; Olmstead, M. M.; Iezzi, E.; Duchamp, J. C.; Dorn, H. C.; Balch, A. L. *J. Am. Chem. Soc.* **2002**, *124*, 3494−3495.

***Table 2.*** Relative Thermodynamic Energies (kcal/mol) and HOMO/LUMO Levels (eV) for $Sc_3N@C_{78}$ *N*-Tritylpyrrolidino Monoadducts

| site of addition | relative thermodynamic energy of $Sc_3N@C_{78}$ *N*-tritylpyrrolidino monoadduct | HOMO level of $Sc_3N@C_{78}$ *N*-tritylpyrrolidino monoadduct | LUMO level of $Sc_3N@C_{78}$ *N*-tritylpyrrolidino monoadduct | HOMO–LUMO gap of $Sc_3N@C_{78}$ *N*-tritylpyrrolidino monoadduct | final MBO for $Sc_3N@C_{78}$[35] |
|---|---|---|---|---|---|
| c-f | 0.00 | −5.28 | −3.11 | 2.17 | 1.280 |
| b-d | 2.13 | −5.23 | −3.11 | 2.13 | 1.271 |
| d-e | 21.89 | −5.02 | −3.51 | 1.51 | 1.097 |
| f-g | 23.50 | −5.10 | −3.33 | 1.77 | 1.165 |

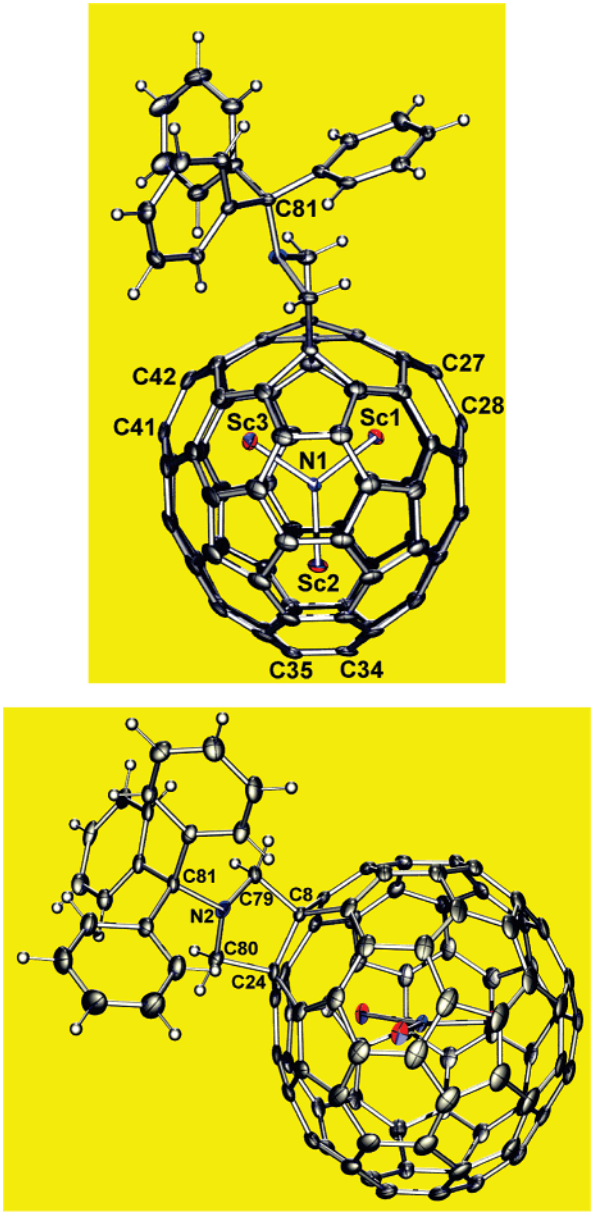


***Figure 6.*** Two drawings of $Sc_3N@C_{78}-(CH_2)_2NC(C_6H_5)_3$, **1a**, with 50% thermal elipsoids. The top view looks down what would be the three-fold axis of the unfunctionalized endohedral, while the lower view is arranged to show the disposition of the addend. The benzene molecules in the solvate are not shown.

and 1.394 Å for the c-f bonds. The c-f bond at the site of additions has been excluded from this averaging. Other average C−C distances are: 1.441 Å for the a-a bonds at 5,6 ring junctions, 1.420 Å for the a-b bonds (5,6 junction), 1.445 Å for the b-c bonds (6,6 junction), 1.468 Å for the d-d bonds (6,6 junction), 1.450 Å for the d-e bonds (6,6 junction), 1.441 Å for the e-g bonds (5,6 junction), 1.429 Å for the f-g bonds (6,6

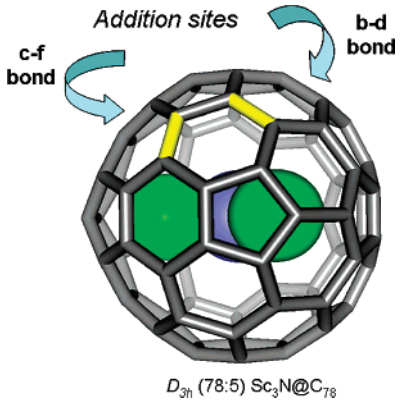


***Figure 7.*** Two addition sites c-f and b-d bond (yellow) on $D_{3h}$ (78:5) $Sc_3N@C_{78}$ cage.

junction), 1.419 Å for the g-g bonds (6,6 junction), 1.443 Å for the h-e bonds (5,6 junctions), and 1.436 Å for the h-h bonds (6,6 junction), which are the carbon atoms nearest the scandium ions.

## Conclusions

In conclusion, we have synthesized and isolated derivatives of $Sc_3N@C_{78}$ via 1,3-dipolar cycloaddition of tritylazomethine ylides. The addition sites of two kinetically stable *N*-tritylpyrrolidino monoadducts **1a** and **1b** were located at c-f and b-d bonds on the $Sc_3N@C_{78}$ cage, respectively (Figure 7), based on NMR spectra and DFT calculations. The single-crystal X-ray diffraction study of $Sc_3N@C_{78}$ derivative **1a** confirms that the addition has occurred at the c-f bond on the ellipsoidal metallofullerene $D_{3h}$ (78:5) $Sc_3N@C_{78}$. The $Sc_3N$ unit remains in the horizontal plane of the $D_{3h}$ (78:5) cage after exohedral derivatization and does not interact directly with the site of addition. This represents the first case (in contrast with earlier studies of $A_3N@C_{80}$ molecules and other endohedral metallofullerenes) where the internal trimetallic cluster ($Sc_3N$) is restricted to a horizontal plane in the molecule and thus demonstrates regiocontrol of adduct docking on a metallofullerene sphere.

## Experimental Section

**Materials and Methods.** A $Sc_3N@C_{68}$, $Sc_3N@C_{78}$, and$Sc_3N@C_{80}$ mixture was obtained by the chemical separation method, as reported in detail earlier.[24] Pure $Sc_3N@C_{78}$ was isolated and purified by HPLC at retention time of 41.2 min (PYE column, 10 × 250 mm, toluene, 2 mL/min). *N*-Tritylpyrrolidino derivatives of $Sc_3N@C_{78}$ were synthesized by heating a solution of 2.0 mg (1.8 $\mu$mol) of $Sc_3N@C_{78}$ and 12.2 mg (37 $\mu$mol) of *N*-triphenylmethyl-5-oxazolidinone in 25 mL of chlorobenzene at reflux for 3 h under $N_2$. The solvent was removed under a stream of nitrogen overnight. The crude solid was dissolved in toluene and then injected into an HPLC for isolation and analysis (PYE column, 10 × 250 mm, toluene, 2 mL/min). On the basis of recovered $Sc_3N@C_{78}$ (~1 mg), we estimate a yield of of ~25%

for each monoadduct (**1a** and **1b**). The HPLC system and the MALDI-TOF mass spectrometer are the same as were used in the previous study.[30] A JEOL ECP 500 MHz instrument was used for $Sc_3N@C_{78}$ NMR measurements.

**Computations.** Full geometry optimizations were conducted at the B3LYP level[37−39] using the Gaussian 03 program.[40] The effective core potential and the corresponding basis set were used for Sc. The basis sets employed were LanL2DZ for Sc,[41] and 3-21G* for C, N, and H.[42] For the computed structure of the c-f bond adduct of $Sc_3N@C_{78}$, we referred to the crystallographic data. As for structures of the b-d, d-e, and f-g bond adducts, we assumed that the functional group would connect to the carbon as far away as possible from the positions of the metal atoms. All the calculations were subjected to frequency analyses, which were performed at the same level as that of the geometry optimization. As a result, no imaginary frequencies are reported for optimized structures.

**Crystals of $Sc_3N@C_{78}$-$(CH_2)_2NC(C_6H_5)_3$·2.5($C_6H_6$)** were obtained by slow evaporation of a benzene solution of the compound. Crystal data for $Sc_3N@C_{78}$-$(CH_2)_2NC(C_6H_5)_3$·2.5($C_6H_6$): black needle, 0.27 × 0.05 × 0.05 mm, triclinic, space group $P\bar{1}$, $a$ = 10.923(2), $b$ = 16.311(3), and $c$ = 18.734(3) Å, α = 75.545(2), $\beta$ = 76.371(2), and $\gamma$ = 77.167(2)°, $V$ = 3093.4(9) Å,$^3$ $\lambda$ = 0.71073 Å, $Z$ = 2, $D_c$ = 1.682 Mg m$^{-3}$; $\mu$(Mo Kα) = 0.391 mm$^{-1}$; $T$ = 90(2) K; Bruker Apex II; scans, 2 max = 66.46°; 25065 reflections collected; min/max transmission = 0.90/0.98; Patterson and difference Fourier methods solution (SHELXS-97, Sheldrick, 1990); full-matrix least-squares based on $F^2$ (SHELXL-97; Sheldrick, 1998); $R$ = 0.1802 for all data; conventional $R_1$ = 0.0679 computed for 9806 observed data (>2$\sigma$($I$)) with 1043 parameters and no restraints.

**Acknowledgment.** We are grateful for support of this work by the National Science Foundation [(CHE-0413857 (A.L.B.), CHE-0443850 (H.C.D.), DMR-0507083 (H.C.D., H.W.G.)] and the National Institutes of Health [1R01-CA119371-01 (H.C.D., H.W.G.)].

**Supporting Information Available:** Complete ref 40; UV−vis spectrum of **1a**; X-ray crystallographic data for $Sc_3N@C_{78}$−$(CH_2)_2N(C(C_6H_5)_3)$·2.5($C_6H_6$) in CIF format. This material is available free of charge via the Internet at http://pubs.acs.org.

JA072345O

(37) Lee, C.; Yang, W.; Parr, R. G. *Phys. Rev. B* **1988**, *37*, 785−789.
(38) Becke, A. D. *Phys. Rev. A* **1988**, *38*, 3098−3100.
(39) Becke, A. D. *J. Chem. Phys.* **1993**, *98*, 5648−5652.
(40) Frisch, M. J.; et al. *Gaussian 03*, revision B.05; Gaussian Inc.: Wallingford, CT, 2004.
(41) Hay, P. J.; Wadt, W. R. *J. Chem. Phys.* **1985**, *82*, 284−298.
(42) Hehre, W. J.; Ditchfield, R.; Pople, J. A. *J. Chem. Phys.* **1972**, *56*, 2257−2261.